

AFST

Annales de la Faculté des Sciences de Toulouse MATHÉMATIQUES

RUDY DISSLER

Relative Trisections of Fiber Bundles over the Circle

Tome XXXIII, n° 5 (2024), p. 1373–1412.

<https://doi.org/10.5802/afst.1801>

© les auteurs, 2024.

Les articles des *Annales de la Faculté des Sciences de Toulouse* sont mis à disposition sous la licence Creative Commons Attribution (CC-BY) 4.0
<http://creativecommons.org/licenses/by/4.0/>



Publication membre du centre
Mersenne pour l'édition scientifique ouverte
<http://www.centre-mersenne.org/>
e-ISSN : 2258-7519

Relative Trisections of Fiber Bundles over the Circle ^(*)

RUDY DISSLER ⁽¹⁾

ABSTRACT. — For an oriented 4-dimensional fiber bundle over S^1 , we build a relative trisection from a sutured Heegaard splitting of the fiber. We provide an algorithm to explicitly construct the associated relative trisection diagram, from a sutured Heegaard diagram of the fiber. As an application, we glue our relative trisection diagrams with existing diagrams to recover trisected closed fiber bundles over S^1 and trisected spun manifolds, and to provide trisections for 4-dimensional open-books.

RÉSUMÉ. — Nous construisons une trisection pour un fibré sur le cercle, orienté et compact, à partir d'un scindement de Heegaard suturé de la fibre. Nous donnons un algorithme pour construire les diagrammes de trisection relatifs associés, à partir d'un diagramme de Heegaard suturé de la fibre. Enfin, nous recollons nos diagrammes à des diagrammes de trisections relatifs déjà existants, retrouvant ainsi les trisections de fibrés sur le cercle fermés, les trisections de variétés *spun*, et produisant des trisections pour les livres ouverts de dimension 4.

1. Introduction

Gay and Kirby's trisection theory describes closed smooth 4-manifolds as unions of simple pieces: 4-dimensional 1-handlebodies glued together in a suitable way. Results of existence and uniqueness (up to a stabilisation move) were established by Gay and Kirby, who also started to decline the concept in a relative setting, giving birth to the notion of relative trisections of compact 4-manifolds [7]. The theory of relative trisections was then developed by Castro, Gay and Pinzón-Caicedo in [3, 4], establishing, as in the closed case, results of existence and uniqueness (up to stabilisation). Examples of

(*) Reçu le 7 août 2023, accepté le 9 octobre 2023.

(1) Institut de Mathématiques de Marseille (I2M), Centre de Mathématiques et Informatique, 39 rue Joliot-Curie, 13453 Marseille Cedex 13, France — rudy.dissler@etu.univ-amu.fr

Article proposé par Francesco Costantino.

closed trisected manifolds in the literature range from classic low-genus trisections in [7, 16], to more complicated constructions, such as trisections of fiber bundle over the circle by Koenig [13], surface bundles over surfaces by Williams [17], or spun manifolds by Meier [15]. In the relative setting, one can find simple examples such as relative trisections of B^4 or $I \times S^3$ in [2], or more complicated examples of disk bundles over the 2-sphere in [3], or surface complements in [12]. In both settings, these concrete examples are essential: not only do they build one's intuition, they also provide answers to pending questions (for instance, Meier's work was used later on in [9] to produce trisections of equal genus of the same manifold that actually need stabilisations before becoming isotopic). The purpose of this article is to construct another class of relative trisections: relative trisections of compact fiber bundles over the circle, in echo of Koenig's constructions in the closed setting [13].

The interest of our constructions is two-fold. First, we build our relative trisections in a very elementary way, inspired from [13], using a sutured Heegaard splitting of the fiber. It is therefore a rather good exercise in manipulating relative trisections, as it shows the complexity resulting from a non-empty boundary and allows to visualize quite precisely what is happening. Second, relative trisections can be glued together, provided that the induced decompositions of the boundaries agree [5]. This gives rise to a (relative) trisection of the resulting space. This fact is used in [5, 12] to build trisections of closed manifolds by gluing relative trisections of their different pieces. In this article, we will use our relatively trisected fiber bundles over the circle to construct trisections of closed fiber bundles over the circle, 4-dimensional open books, and spun manifolds.

Let's focus on our bundle: the base is a circle and the fiber is a compact 3-manifold with non-empty boundary. The differentiable structure on the bundle is the product one, inherited from the unique differentiable structures on the base and on the fiber. The main idea is to consider a sutured Heegaard splitting of the fiber that is either preserved or flipped by the monodromy of the bundle (which roughly means that the monodromy sends each compression body of the splitting to itself in the first case, and flips the compression bodies in the second). From this specific sutured Heegaard splitting, we will derive a relative trisection of the bundle, by combining the decomposition of the fiber given by the splitting with a decomposition of the base into intervals, using a technique of tubing. We will also show that there always exists a sutured Heegaard splitting of the fiber that is preserved by the monodromy. Therefore, there always exists a preserved sutured Heegaard splitting from which to derive a relative trisection; however, we also consider — and actually start with — the case of a flipped splitting because

it is simpler and produces a lower genus trisection. The boundary of the fiber can be disconnected, but the action of the monodromy on its components complicates the computation of the genus of the relative trisection. These results are condensed in the following theorems.

THEOREM 1.1. — *Let M be a smooth, compact, oriented, connected 3-manifold, and ϕ an orientation preserving self-diffeomorphism of M . Then M admits a sutured Heegaard splitting $M = C_1 \cup_S C_2$ that is preserved by ϕ , i.e. there is an ambient isotopy of M that sends C_1 to $\phi(C_1)$ and C_2 to $\phi(C_2)$.*

By *ambient isotopy*, we mean an isotopy $F : M \times [0, 1] \rightarrow M$ such that $F(\cdot, 0) = \text{Id}_{|M}$ and, denoting by f_i the embedding of C_i in M , $F(f_i, 1) = \phi \circ f_i$.

Remark 1.2. — Theorem 1.1 can be proven using triangulations, but we will stick to the differential category in our proof through Morse functions.

THEOREM 1.3. — *Let M be a smooth, compact, oriented, connected 3-manifold and ϕ an orientation-preserving self-diffeomorphism of M . Let X be the smooth oriented bundle over the circle with fiber M and monodromy ϕ . Suppose that M admits a sutured Heegaard splitting $M = C_1 \cup_S C_2$ that is flipped by ϕ , with S a compact surface with b boundary components and Euler characteristic $\chi(S)$. Then X admits a relative trisection $X = X_1 \cup X_2 \cup X_3$, where the Euler characteristic of $X_1 \cap X_2 \cap X_3$ is $3(\chi(S) - b)$.*

THEOREM 1.4. — *Let M be a smooth, compact, oriented, connected 3-manifold and ϕ an orientation-preserving self-diffeomorphism of M . Let X be the smooth oriented bundle over the circle with fiber M and monodromy ϕ . Then M admits a sutured Heegaard splitting that is preserved by ϕ . Given such a splitting, we denote by S its Heegaard surface, with b boundary components and Euler characteristic $\chi(S)$. Then X admits a relative trisection $X = X_1 \cup X_2 \cup X_3$, where the Euler characteristic of $X_1 \cap X_2 \cap X_3$ is $6(\chi(S) - b)$.*

The paper is organised as follows. Section 2 reviews the notions of sutured Heegaard splittings of compact 3-manifolds, relative trisections of compact 4-manifolds, as well as the associated diagrams. For a more thorough approach, the reader may refer to [3, 4]. In Section 3, we make a detour in dimension 3 to prove Theorem 1.1, which shows that we can always find a sutured Heegaard splitting of the fiber that is preserved, up to isotopy, by the monodromy. In Section 4, we build our relative trisections of fiber bundles over the circle, provided that the fiber admits a sutured Heegaard splitting either preserved or flipped by the monodromy of the bundle. We compute the

parameters of these relative trisections, giving more precise versions of Theorems 1.3 and 1.4. In Section 5, we describe the corresponding diagrams. In Section 6, we use a gluing technique to construct trisection diagrams of some classes of closed manifolds from our relative trisection diagrams. First, we recover the trisected closed fiber bundle over the circle in [13], then the trisected spun manifolds in [15]; finally we provide a new class of trisections: trisected

4-dimensional open-books, whose fiber is a 3-manifold with boundary a torus. More specifically, we explicitly derive a $(6g + 4)$ -trisection diagram for the open-book from a genus g sutured Heegaard diagram of the fiber.

2. Background

We denote by $F_{g,b}$ a compact connected surface of genus g with b boundary components. We say that two decompositions of a manifold $M = \bigcup M_i$ and $M = \bigcup M'_i$ are isotopic if there is an ambient isotopy of M taking each M_i to M'_i .

DEFINITION 2.1. — *Let S be a compact connected surface with non-empty boundary. Take the product $S \times [0, 1]$ and add 3-dimensional 2-handles along a family α of disjoint, non trivial simple closed curves on $S \times \{0\}$. Call C the resulting compact, connected 3-manifold. We say that C is a compression body and define:*

- *its positive boundary $\partial_+ C$ as $S \times \{1\}$;*
- *its negative boundary $\partial_- C$ as $\partial C \setminus ((\partial S \times]0, 1[) \cup \partial_+ C)$.*

We say that the set α is a cut system of S corresponding to C .

Thus $\partial_- C$ is obtained by compressing $\partial_+ C$ along the α curves. Throughout this article, we will only consider negative boundaries with no closed components. In this case, a compression body is a standard handlebody with a fixed decomposition of its boundary.

Remark 2.2. — We can also reverse the construction and obtain a compression body from its negative boundary $\partial_- C = F$, a compact (possibly disconnected) surface, by taking the product $F \times [0, 1]$ and adding 3-dimensional 1-handles along $F \times \{1\}$ so that the resulting 3-manifold C is connected. In this perspective the negative boundary is $\partial_- C = F \times \{0\}$ and the positive boundary $\partial_+ C$ is set as the closure of $\partial C \setminus ((F \times \{0\}) \cup (\partial F \times [0, 1]))$ (see Figure 2.1).

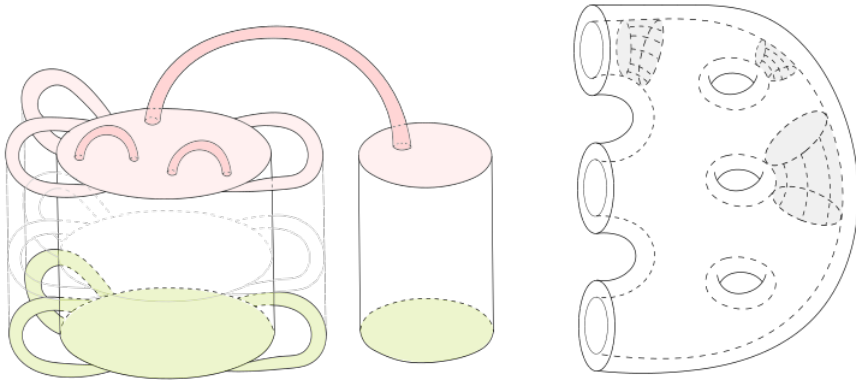


Figure 2.1. Two representations of a compression body. Left: negative boundary in green and positive boundary in pink; 1-handles in dark pink. Right: positive boundary in plain and negative boundary in dashed; 2-handles in grey.

We will use handlebodies with a compression body structure to produce decompositions of compact 3-manifolds with non-empty boundary. For that purpose, we need the concept of sutured manifold, introduced by Gabai in [6]. In what follows, we just keep the necessary amount of theory.

DEFINITION 2.3. — *Let M be a compact, smooth, connected 3-manifold with non-empty boundary. A sutured Heegaard splitting of M is a decomposition $M = C_1 \cup_S C_2$, where:*

- *the intersection $S = C_1 \cap C_2$ is a compact connected surface with non-empty boundary;*
- *C_1 and C_2 are handlebodies with a compression body structure, such that $\partial_+ C_1 = -\partial_+ C_2 = S$.*

We say that a sutured Heegaard splitting of M is balanced if $\partial_- C_1 \simeq \partial_- C_2$.

Remark 2.4. — A sutured Heegaard splitting of M induces a decomposition of ∂M into two compact surfaces with non-empty boundary S_1 and S_2 and a finite set of annuli $\bigcup_i A_i$ joining each component of ∂S_1 to a component of ∂S_2 . We call such a decomposition a *sutured decomposition* of ∂M .

Remark 2.5. — Necessarily $\bigcup_i A_i \simeq (\partial S_1 \times [0, 1]) \simeq (\partial S_2 \times [0, 1])$. A curve on a A_i isotopic to a component of ∂S_1 is called a *suture* of the decomposition. Sometimes in this article, we will not need to differentiate a sutured decomposition of a surface S from a decomposition into two compact surfaces glued along their common boundary. When that is the case, we will also refer to the latter as a sutured decomposition of S .

We now move to dimension 4. We will just briefly define relative trisections: for proofs and more details, we refer to [2, 3, 4].

DEFINITION 2.6. — *A relative trisection of a compact, connected, smooth 4-manifold X is a decomposition $X = X_1 \cup X_2 \cup X_3$ such that:*

- *each X_i is a 4-dimensional handlebody, i.e. $X_i \simeq \natural^{k_i}(S^1 \times B^3)$ for some k_i ;*
- *the triple intersection $X_1 \cap X_2 \cap X_3 = S$ is a compact connected surface with boundary;*
- *each intersection $(X_i \cap X_j) \cap \partial X$ is diffeomorphic to a given compact surface P ;*
- *each double intersection $X_i \cap X_j = (\partial X_i \cap \partial X_j)$ is a handlebody $C_{i,j}$ with a compression body structure defined by $\partial_+ C_{i,j} = S$ and $\partial_- C_{i,j} = (X_i \cap X_j) \cap \partial X \simeq P$;*
- *each $X_i \cap \partial X$ is diffeomorphic to $P \times I$.*

Definition 2.6 induces a decomposition of ∂X into:

- three sets diffeomorphic to $P \times I$, glued together to form a P -fiber bundle over the circle;
- solid tori $\partial P \times I \times I$ glued trivially so as to fill each boundary component of the bundle.

This is an open-book decomposition of ∂X , with page P and binding $\partial P \simeq \partial S$.

We call the triple intersection the *central surface* of the trisection. If the boundary of X is connected, a (g, k_1, k_2, k_3, p, b) -relative trisection is a relative trisection involving a central surface of genus g with b boundary components, 4-dimensional handlebodies of genus k_i and pages of genus p (if all the k_i 's are equal to k , we will simply write a (g, k, p, b) -relative trisection). If ∂X is not connected, then there are as many pages as components in ∂X . In this case we will use multi-indices as p and b , and notice that the sum of the indices in b must be equal to the number of boundary components of the central surface.

One key feature of sutured Heegaard splittings and relative trisections is that they can both be described by diagrams, just as Heegaard splittings and trisections.

DEFINITION 2.7. — *A sutured Heegaard diagram is a triple (S, α, β) , where S is a compact connected surface with boundary and α and β are two sets of disjoint, non-trivial simple closed curves in $\text{Int}(S)$, such that compressing S along each set does not produce any closed component.*

Each set thus corresponds to a cut system for some compression body, and the last condition ensures that this compression body is also a handlebody. Therefore, a sutured Heegaard diagram defines a 3-manifold with a sutured Heegaard splitting. We can reverse the process and obtain a sutured Heegaard diagram from a sutured Heegaard splitting, by setting S as the intersection $C_1 \cap C_2$, the α 's (resp. the β 's) as a cut system defining C_1 (resp. C_2). Actually, there is a one-to-one correspondence between sutured Heegaard diagrams (up to diffeomorphism of the surface and handleslides of curves within each cut system) and sutured Heegaard splittings (up to diffeomorphism).

Example 2.8. — Given a Heegaard diagram (Σ, α, β) (associated to a closed 3-manifold M), consider the sutured Heegaard diagram (S, α, β) , where S is Σ minus the interior of b disks disjoint from the α and β curves. If $b = 1$, we obtain a sutured Heegaard diagram associated to M minus the interior of a 3-ball; if $b = 2$, we obtain a sutured Heegaard diagram associated to M minus the interior of a solid torus. If $b = 2$ and we add one curve parallel to a boundary component to the α 's or the β 's, we obtain again M minus the interior of a 3-ball; if $b = 2$ and we add to each set a curve parallel to a boundary component, the result is M minus the interior of two disjoint 3-balls.

DEFINITION 2.9. — A standard sutured Heegaard diagram is the connected sum of standard genus 1 Heegaard diagrams of S^3 and $S^1 \times S^2$ and a compact surface with non-empty boundary $F_{p,b}$.

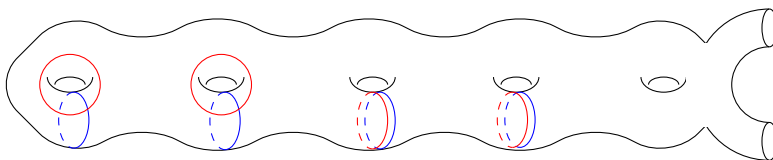


Figure 2.2. A standard sutured Heegaard diagram

DEFINITION 2.10. — A relative trisection diagram is a 4-tuple $\{S, \alpha, \beta, \gamma\}$, where each triple $\{S, \alpha, \beta\}$, $\{S, \beta, \gamma\}$, $\{S, \alpha, \gamma\}$ is handleslide-diffeomorphic to a standard sutured Heegaard diagram involving the same compact surface $P \simeq F_{p,b}$.

There is a one-to-one correspondence between relative trisection diagrams (up to handleslides of curves within each family α , β and γ and

diffeomorphism of S) and relatively trisected 4-manifolds (up to diffeomorphism), see [3]. If a relative trisection diagram corresponds to a relative trisection $X = X_1 \cup X_2 \cup X_3$, each sutured diagram consisting of the trisection surface and two sets of curves corresponds to a sutured Heegaard diagram of one $(X_{i-1} \cap X_i) \cup (X_i \cap X_{i+1})$.

3. A monodromy-preserved decomposition of M

We want to show that no assumption has to be made on M to find a sutured Heegaard splitting that is preserved by the monodromy. This is the content of Theorem 1.1, which we are now going to prove. To do so, we need some preliminary results.

PROPOSITION 3.1. — *Given a sutured decomposition of ∂M , there exists a sutured Heegaard splitting $M = C_1 \cup_S C_2$ inducing it.*

Proof. — We will use a handle decomposition given by a Morse function. We denote the sutured decomposition of the boundary of M by $\partial M \simeq S_1 \cup (\partial S_1 \times [0, 1]) \cup S_2$ and consider a collar neighbourhood ν of ∂M , $\nu = \psi((S_1 \cup (\partial S_1 \times [0, 1]) \cup S_2) \times [0, 1/2])$, with ψ an embedding such that $\psi((S_1 \cup (\partial S_1 \times [0, 1]) \cup S_2) \times \{0\}) = \partial M$. We define the following smooth function f on ∂M :

- on $\psi(S_1 \times \{0\})$, $f \equiv -1$; on $\psi(S_2 \times \{0\})$, $f \equiv 4$;
- for $((x, u), 0) \in (\partial S_1 \times [0, 1]) \times \{0\}$, $f(\psi((x, u), 0)) = g(u)$, where g is a smooth, strictly increasing function from $[0, 1]$ to $[-1, 4]$ that verifies: $g(0) = -1$, $g(1) = 4$, and $g^{(k)}(0) = g^{(k)}(1) = 0$ for $k > 0$.

Then we extend f to a smooth function \tilde{f} on ν by:

- $\tilde{f}(\psi(y, t)) = t - 1$ for $(y, t) \in S_1 \times [0, 1/2]$ and $\tilde{f}(\psi(y, t)) = -t + 4$ for $(y, t) \in S_2 \times [0, 1/2]$;
- for $((x, u), t) \in (\partial S_1 \times [0, 1]) \times [0, 1/2]$, $\tilde{f}(\psi((x, u), t)) = th(u) + g(u)$, where h is a smooth strictly decreasing function from $[0, 1]$ to $[-1, 1]$ such that:
 - $h(0) = 1$; $h(1/2) = 0$; $h(1) = -1$;
 - $h^{(k)}(0) = h^{(k)}(1) = 0$ for $k > 0$;
 - $-h'(u) < 2g'(u)$ for $0 < u < 1$.

Then \tilde{f} is a smooth function with no critical point on ν , that sends $\psi(\partial M \times \{1/2\})$ to $[-0.5, 3.5]$. As $\psi(\partial M \times \{1/2\})$ is embedded in M , we can use slice charts to extend \tilde{f} to M and finally obtain a smooth function on M , with no critical points on ν , that sends $M \setminus \nu$ to $[-0.5, 3.5]$. We can use a generic Morse

approximation of this function, then modify it around its critical points (therefore, away from ν) to obtain a self-indexing Morse function F . Consider a critical point of index 0. It corresponds to adding a 0-handle, but, as M is connected, there must be a cancelling 1-handle. The same applies to the components of $F^{-1}(\{-1\}) = S_1$, that must be connected by 1-handles. Therefore, the preimage $F^{-1}([-1, 3/2]) = C_1$ is diffeomorphic to the connected union of $F^{-1}(\{-1\}) \times I$ and 1-handles: it is a handlebody with a compression body structure given by $\partial_- C_1 = S_1$ and $\partial_+ C_1 = F^{-1}(\{3/2\}) = S$, where S is a compact connected surface with boundary. By applying the same argument to $-F$, we see that $C_2 = F^{-1}([3/2, 4])$ is also a handlebody with a compression body structure given by $\partial_- C_2 = S_2$ and $\partial_+ C_2 = F^{-1}(\{3/2\}) = S$. Therefore $M = C_1 \cup_S C_2$ is a sutured Heegaard splitting of M , inducing the requested sutured decomposition of ∂M . \square

Remark 3.2. — These arguments are standardly used to prove the handle decomposition theorem and the existence of Heegaard splittings (see for instance [14]). We simply adapted them to the setting created by a sutured decomposition of the boundary. Notice that the gradient of f can be made parallel to ∂M in $\psi(\partial S_1 \times [0, 1])$ for some metric, which is important to understand that $F^{-1}([-1, 0])$ is a thickening of S_1 (with perhaps some extra 3-balls) respecting the sutures (see [1]). We also refer to [10]: this latter article actually covers the proof, but we found it useful to give our version, as [10] focuses on balanced sutured Heegaard diagrams. In this paper, we do not need the full diagrammatic approach of [10], but we do need to work with non balanced decompositions.

DEFINITION 3.3. — *A Morse function $f : M \rightarrow [-1, 4]$ is compatible with a sutured Heegaard splitting $M = C_1 \cup_S C_2$ if:*

- *we have $f^{-1}([-1, 3/2]) = C_1$, $f^{-1}([3/2, 4]) = C_2$, and $f^{-1}(3/2) = S$;*
- *the critical points of f of index 0 and 1 belong to C_1 and the critical points of index 2 and 3 belong to C_2 .*

Now we prove that *any* sutured Heegaard splitting can be given by a compatible Morse function.

PROPOSITION 3.4. — *If $M = C_1 \cup_S C_2$ is a sutured Heegaard splitting, then there is a Morse function compatible with it.*

Proof. — We set $V_1 = \partial_- C_1 \setminus \nu_1$, where ν_1 is a small regular neighbourhood of $\partial(\partial_- C_1)$ in $\partial_- C_1$. Consider a handle H glued to $V_1 \times [0, 1]$. We write T a regular neighbourhood of the attaching sphere of H in $V_1 \times [0, 1]$. Then there is a Morse function G on $(V_1 \times [0, 1]) \cup H$ such that $G(x, t) = t$ outside of the subset $H \cup T$, with only one critical point corresponding to the attachment of H . Considering the handles to be attached separately, we combine

such functions into a Morse function F on the union of $V_1 \times [0, 1]$ and of the 1-handles of the splitting, with critical points of index 1 corresponding to the attachment of the 1-handles. We can apply the same argument to C_2 considered as the union of $\partial_- C_2 \times I$ and 1-handles, then take the opposite Morse function to produce a Morse function with critical points corresponding to the 2-handles, equal to 4 on the intersection with ∂M and agreeing with F on S . Combining the two functions gives a Morse function corresponding to the handle decomposition on $C_1 \cup C_2$ minus a regular neighbourhood of $\partial S \times I$. Finally we interpolate between the values on $\partial V_1 \times [0, 1]$ and the values defined on $\partial(\partial_- C_1)$ for the Morse function of Proposition 3.1 without creating new critical points, which produces the desired Morse function on M . \square

PROPOSITION 3.5. — *If two sutured Heegaard splittings of a manifold $M = C_1 \cup_S C_2$ and $M = C'_1 \cup_{S'} C'_2$ induce the same sutured decomposition of ∂M , then they become isotopic after a finite sequence of interior stabilisations.*

Proof. — Using Proposition 3.4, let f (resp. f') be a Morse function defining $M = C_1 \cup_S C_2$ (resp. $M = C'_1 \cup_{S'} C'_2$). We can assume that f and f' agree on a neighbourhood of ∂M (see the proof of Proposition 3.4). Then Cerf theory produces a path of generalised ordered Morse functions $\{f_t\}_{t \in [0, 1]}$ from $f = f_0$ to $f' = f_1$. As f_0 and f_1 do not have critical points on a regular neighbourhood of ∂M , we can assume that the f_t 's behave accordingly, and that they agree with f_0 and f_1 on this neighbourhood, therefore fixing the sutured decomposition of ∂M . Now we can apply standard arguments of Cerf theory and handle decompositions (see [10]): as t moves from 0 to 1, the f_t will produce a finite number of births and deaths of critical points, which correspond to stabilisations and destabilisations, as well as a finite number of handleslides. \square

Now we need another proposition, which relies on more combinatorial arguments, and will allow us to conclude our proof of Theorem 1.1.

PROPOSITION 3.6. — *If M is a compact oriented connected 3-manifold with boundary, and ϕ is an orientation preserving self-diffeomorphism of M , then there exists a sutured decomposition of ∂M that is preserved by a diffeomorphism of M isotopic to ϕ .*

Proof. — Pick a component $\partial_1 M$ of ∂M , and choose a disk $D_1 \subset \partial_1 M$. Now, let's consider the orbit of $\partial_1 M$ under the action of ϕ :

$$\{\partial_1 M, \dots, \partial_j M = \phi(\partial_{j-1} M) = \phi^{j-1}(\partial_1 M), \dots, \partial_s M = \phi^{s-1}(\partial_1 M) = \phi^{-1}(\partial_1 M)\}.$$

Then $\phi^s(D_1)$ is not necessarily D_1 , but we can compose $\phi|_{\partial M}$ with a diffeomorphism g of ∂M equal to the identity on every component other than $\partial_1 M$, and isotopic to the identity on $\partial_1 M$ but sending $\phi^s(D_1)$ to D_1 . As g is isotopic to the identity on ∂M , we can extend it to a diffeomorphism of M isotopic to the identity, that we still call g . Then $g \circ \phi$ is a diffeomorphism of M isotopic to ϕ that preserves the set $\{D_1, D_2 = \phi(D_1), \dots, D_s = \phi^{s-1}(D_1)\}$. By setting a sutured decomposition of each component:

$$\partial_j M = D_j \cup (\partial D_j \times [0, 1]) \cup \overline{(\partial_j M \setminus (D_j \cup (\partial D_j \times [0, 1])))}$$

we obtain a sutured decomposition of the orbit of $\partial_1 M$ that is preserved by $g \circ \phi$. Now we can apply the same argument on each orbit of the action of ϕ on ∂M , as g leaves these orbits invariant. We have thus produced the desired sutured decomposition of ∂M . \square

Proof of Theorem 1.1. — Let ϕ be an orientation preserving self-diffeomorphism of M . According to Proposition 3.6, we may assume that there is always a sutured decomposition of ∂M that is preserved by ϕ (to be precise, an unbalanced sutured decomposition, see Remark 3.2). Then by Proposition 3.1 there is a sutured Heegaard splitting $M = C_1 \cup_S C_2$ inducing this decomposition. Now we can transpose to the sutured setting the argument of [13]: the image $M = \phi(C_1) \cup_{\phi(S)} \phi(C_2)$ is also a sutured Heegaard splitting of M , involving the same decomposition of ∂M . Using Proposition 3.5 (and the fact that the image of a stabilisation is a stabilisation of the image), we can conclude that, after a number of interior stabilisations, we always obtain a sutured Heegaard splitting that is preserved by ϕ , up to isotopy. \square

Remark 3.7. — Suppose that ϕ flips a balanced sutured decomposition of ∂M . A natural question would be: does ϕ flip a sutured Heegaard splitting of M inducing this decomposition? This question is open, because the proof of Proposition 3.5 relies on the fact that the decomposition of ∂M is *preserved* by ϕ . In the closed case, however, the answer is positive, and much easier, because any Heegaard splitting is flippable, up to stabilisations.

4. Constructing the relative trisections

Given a compact, oriented, connected, smooth 3-manifold M with non-empty boundary (possibly disconnected), together with an orientation preserving self-diffeomorphism ϕ , we consider the fiber bundle $X = (M \times I)/\sim$, where $(x, 0) \sim (\phi(x), 1)$. Then X is a smooth, compact, oriented, connected 4-manifold (with non-empty boundary), of which we want to build a relative trisection.

We suppose that M admits a sutured Heegaard splitting $M = C_1 \cup_S C_2$ that ϕ preserves (i.e. $\phi(C_i) = C_i$) or flips (i.e. $\phi(C_i) = C_{i+1}$, considering indices modulo two). We denote by g the genus of S and by b its number of boundary components, i.e. $S \simeq F_{g,b}$. According to Theorem 1.1, we can always expect M to admit a sutured Heegaard splitting that is preserved, up to isotopy, by ϕ (the fact that it is only preserved up to isotopy is not a problem because isotopic monodromies produce diffeomorphic bundles).

Remark 4.1. — The monodromy acts on the components of both ∂M and ∂S ; in either case it can preserve or flip boundary components. We don't make any assumptions on how the monodromy acts on the boundary components in what follows, unless otherwise stated.

4.1. Case 1: ϕ flips a sutured Heegaard splitting of M

In this case, necessarily $\partial_- C_1 \simeq \partial_- C_2$, i.e. $M = C_1 \cup_S C_2$ is balanced. We can represent X as a rectangle with vertical edges identified, as in Figure 4.1. The horizontal segment corresponds to the interval I parametrized by t . Each vertical segment is a copy of M . The vertical segments $M \times \{0\}$ and $M \times \{1\}$ are identified according to ϕ .

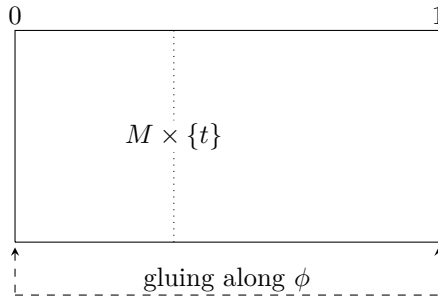


Figure 4.1. A representation of X

Next we divide each copy $M \times \{t\}$ according to $(C_1 \cup_S C_2) \times \{t\}$. We further divide the horizontal segment I , keeping in mind that C_i is identified with C_{i+1} at $0 \sim 1$, to obtain the decomposition represented on Figure 4.2.

Now, each X'_k on Figure 4.2 is diffeomorphic to a $C_i \times I$. Because the C_i 's are tridimensional handlebodies, the X'_k 's are 4-dimensional handlebodies. But the triple intersection is not connected. So we still have a bit of work

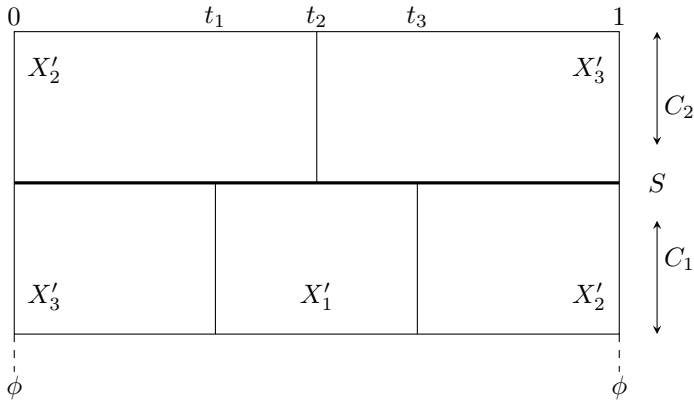


Figure 4.2. A decomposition of X .

to do: the last step is to drill out three sets of 4-dimensional tubes $I \times B^3$ along the boundary of the X'_k 's, then assign each set of tubes to one X'_k , giving the final decomposition of Figure 4.3. The global construction is the same as in the closed case ([13]), but because of the boundary, we have to be more careful as to how we design our tubes.

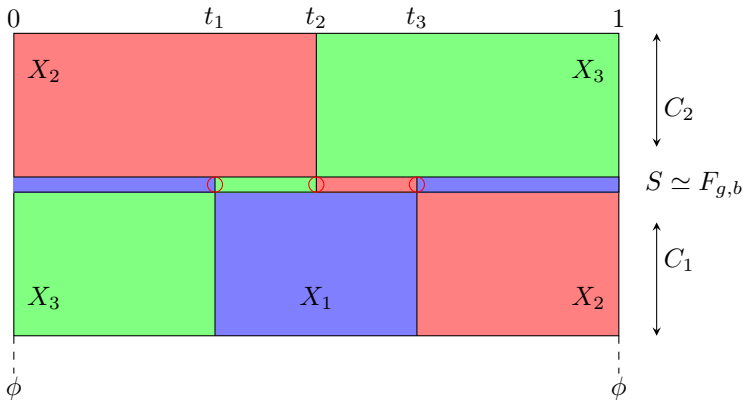


Figure 4.3. A trisection of X , case 1.

Let's focus on the horizontal narrow coloured stripes dividing the rectangle in Figure 4.3. Every stripe represents a set of b 4-dimensional tubes, i.e. copies of $I \times B^3$. So each tube can be seen as a family of 3-balls $\{B_t\}$,

parametrized by t . We impose that, for each t , B_t intersects $S \times \{t\}$. Now we must specify *how*. For instance, if each B_t intersects $S \times \{t\}$ on the interior of the surface, the pages $(X_i \cap X_j) \cap \partial X$ are never connected.

- We start with a tube $[t_1, t_2] \times B^3$. We choose a component of ∂S that we call $\partial_1 S$. Then we define, for each $t \in [t_1, t_2]$, a ball B_t intersecting $S \times \{t\}$ along a disk, $\partial_1 S \times \{t\}$ along a closed interval and $\partial M \times \{t\}$ along a disk. Thus we create a path of 3-balls $\{B_t^{3,1} \mid t \in [t_1, t_2]\}$. We impose that this path is smooth and set it as our first tube $T_{3,1}$. We define in the same fashion a tube $T_{2,1}$ in $M \times [t_2, t_3]$.
- Then we design a quotient tube $T_{1,1} = ([t_3, 1] \cup_{0 \sim 1} [0, t_1]) \times B^3$, by gluing two tubes $\{B_t^{1,1} \mid t \in [t_3, 1]\}$ and $\{B_t^{1,1} \mid t \in [0, t_1]\}$ at $0 \sim 1$.
- We impose that:
 - all the tubes are disjoint;
 - $B_{t_1}^{1,1} \subset C_1 \times \{t_1\}$ and $B_{t_3}^{1,1} \subset C_1 \times \{t_3\}$;
 - $B_{t_2}^{2,1} \subset C_2 \times \{t_2\}$ and $B_{t_3}^{2,1} \subset C_1 \times \{t_3\}$;
 - $B_{t_1}^{3,1} \subset C_1 \times \{t_1\}$ and $B_{t_2}^{3,1} \subset C_2 \times \{t_2\}$;
 - for each $t_i < t < t_{i+1}$, $S \times \{t\}$ is transverse to $B_t^{k,1}$.
- We define $3b$ tubes $\{T_{1,1} \dots T_{1,b}\}$, $\{T_{2,1} \dots T_{2,b}\}$, $\{T_{3,1} \dots T_{3,b}\}$ in the same way, for each of the b components of ∂S . We set $X_k = (X'_k \cup (\bigcup_{l \in [1,b]} T_{k,l})) \setminus \text{Int}(\bigcup_{i \neq k} \bigcup_{l \in [1,b]} T_{i,l})$.

Informally, the 3-balls constituting each tube begin their path in $\{t_i\}$ fully included in $C_1 \times \{t_i\}$ or $C_2 \times \{t_i\}$, then move transversely to S to the position occupied in $\{t_{i+1}\}$ (see Figure 4.4). All this allows us to get a compact surface for $(X_i \cap X_j) \cap \partial X$.

Remark 4.2. — The number of tubes allows the number of boundary components of the pages to match that of the central surface (and the number of boundary components of ∂X).

Remark 4.3. — The 3-balls do not affect, up to diffeomorphism, the C_i 's, nor the surfaces S and $\partial_- C_i$. Therefore, we will simply refer to a C_i minus the interior of the family of 3-balls defined above as a C_i , and to $(S \times \{t\}) \setminus \text{Int}((S \times \{t\}) \cap \bigcup_{k,l} B_t^{k,l})$ as $(S \times \{t\})$.

PROPOSITION 4.4. — *The decomposition $X = X_1 \cup X_2 \cup X_3$ is a relative trisection of X .*

Proof. — We just need to check that the pieces of the decomposition corresponds to those defined in Definition 2.6.

- Each X_k is a union of a 4-dimensional handlebody $C_i \times I$ and b 4-dimensional 1-handles (our tubes $\bigcup_{l \in [1,b]} T_{k,l}$). Therefore each X_k is a 4-dimensional handlebody.

Relative Trisections of Fiber Bundles over the Circle

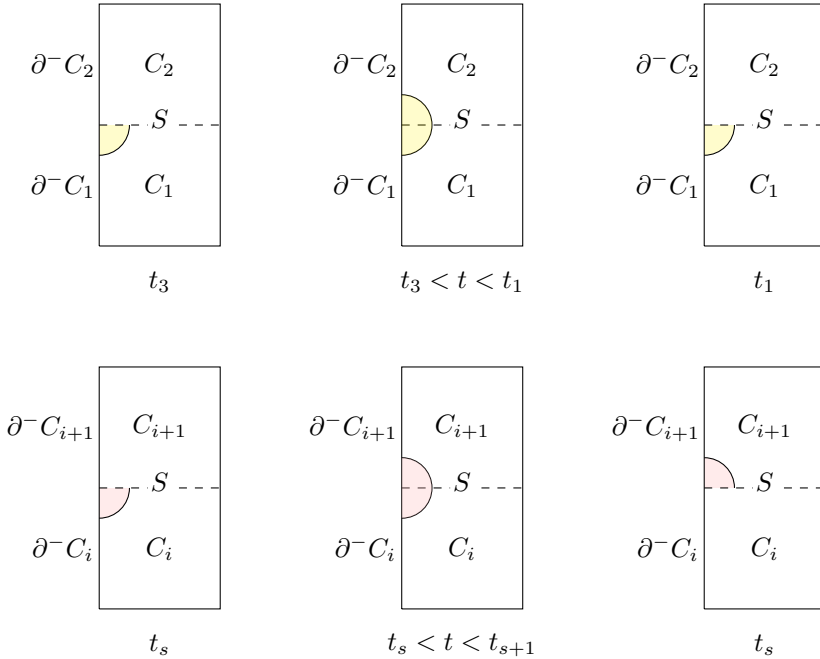


Figure 4.4. Visualising the positions of the 3-balls on the compression bodies. With a yellow $B_{1,l}$ and a pink $B_{2,l}$ or $B_{3,l}$.

- The triple intersection $X_1 \cap X_2 \cap X_3$ is composed of three copies of S (the $S \times \{t_i\}$ for $i = 1, 2, 3$), whose boundary components are joined by $3b$ 2-dimensional 1-handles $(B_i^{k,l} \cap (S \times \{t\})) \times I$, as shown on Figure 4.5 and Figure 4.6. So $X_1 \cap X_2 \cap X_3$ is a compact connected surface with non empty boundary.
- The intersection $(X_1 \cap X_2) \cap \partial X$ is a boundary connected sum of $\partial^- C_1 \times \{t_3\}$ and bands (see Figure 4.7 and Figure 4.8). Therefore it is also a compact surface. The other intersections $(X_2 \cap X_3) \cap \partial X$ and $(X_3 \cap X_1) \cap \partial X$ are built in the same way: all three surfaces are diffeomorphic. Note that they can be disconnected if ∂M is disconnected. In this case, they have the same number of components as ∂X (if the monodromy glues together two different boundary components of M , it will act on the pages accordingly).
- As $X_1 \cap X_2$ is composed of:
 - $C_1 \times \{t_3\}$;
 - $S \times [t_1, t_2]$ (a tridimensional handlebody, since S has boundary);
 - $2b$ tridimensional 1-handles linking the above handlebodies;

it is a tridimensional handlebody, that we will call $C_{1,2}$ (see Figure 4.7). Moreover, Figure 4.8 and Figure 4.9 depict the decomposition of the boundary of $X_1 \cap X_2$ as:

$$\partial(X_1 \cap X_2) = (X_1 \cap X_2 \cap X_3) \cup ((X_1 \cap X_2) \cap \partial X)$$

This gives $C_{1,2}$ a structure of compression body, with $\partial_+ C_{1,2} = X_1 \cap X_2 \cap X_3$ and $\partial_- C_{1,2} = (X_1 \cap X_2) \cap \partial X$.

The intersections $X_2 \cap X_3$ and $X_3 \cap X_1$ are built in the same way.

- Finally, we have:

$$\begin{aligned} X_1 \cup \partial X &\simeq (\partial_- C_1 \times [t_1, t_3]) \cup \left(\left(\bigcup_{l \in [1, b]} T_{1, l} \right) \cup \partial X \right) \\ &\simeq ((X_1 \cap X_2) \cap \partial X) \times I \end{aligned}$$

and $X_2 \cap \partial X$ or $X_3 \cap \partial X$ are built in the same way.

Therefore $X = X_1 \cup X_2 \cup X_3$ is a relative trisection of X . □

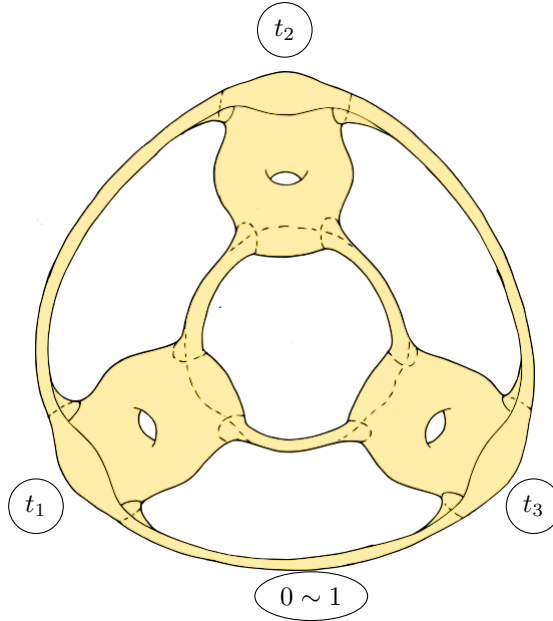


Figure 4.5. A view of $X_1 \cap X_2 \cap X_3$. Case 1: ϕ preserves the components of ∂S .

We can now prove the following result (a more precise but somewhat more engaging version of Theorem 1.3).

THEOREM 4.5. — *Let M be a smooth, compact, oriented, connected 3-manifold and ϕ an orientation-preserving self-diffeomorphism of M . Let X be the smooth oriented bundle over the circle with fiber M and monodromy ϕ . The monodromy acts by permutation on the connected components $\{\partial^1 M, \dots, \partial^{\ell_M} M\}$ of ∂M , and we call $\sigma_{\phi, \partial M}$ this action. Suppose that M admits a sutured Heegaard splitting $M = C_1 \cup_S C_2$ that is flipped by ϕ . We set the following notations:*

- *the surface S is of genus g with b boundary components;*
- *we write p the sum of the genera of the components of $\partial_- C_1 \simeq \partial_- C_2$;*
- *the orbits of $\sigma_{\phi, \partial M}$ are $\{\mathcal{O}_1, \dots, \mathcal{O}_{\ell_X}\}$, where ℓ_X is the number of boundary components of X ; we write p_k the sum of the genera of the components of $\partial_- C_1$ (or equivalently of $\partial_- C_2$) within \mathcal{O}_k and b_k*

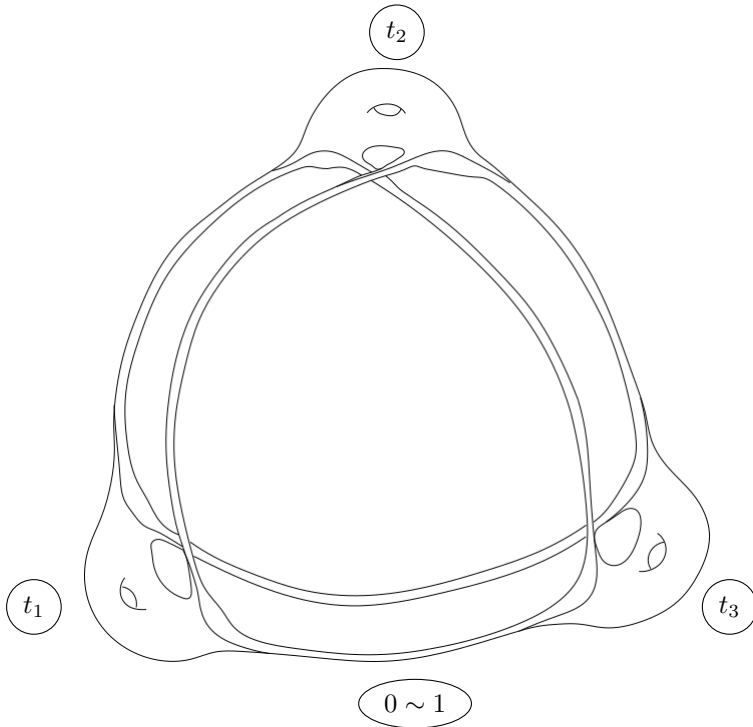


Figure 4.6. A view of $X_1 \cap X_2 \cap X_3$. Case 1: when ϕ flips the components of ∂S .

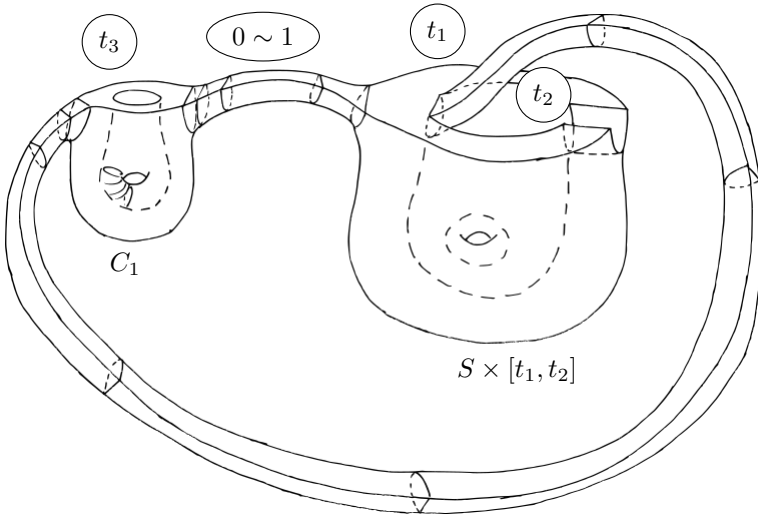


Figure 4.7. A view of $X_1 \cap X_2$. Case 1.

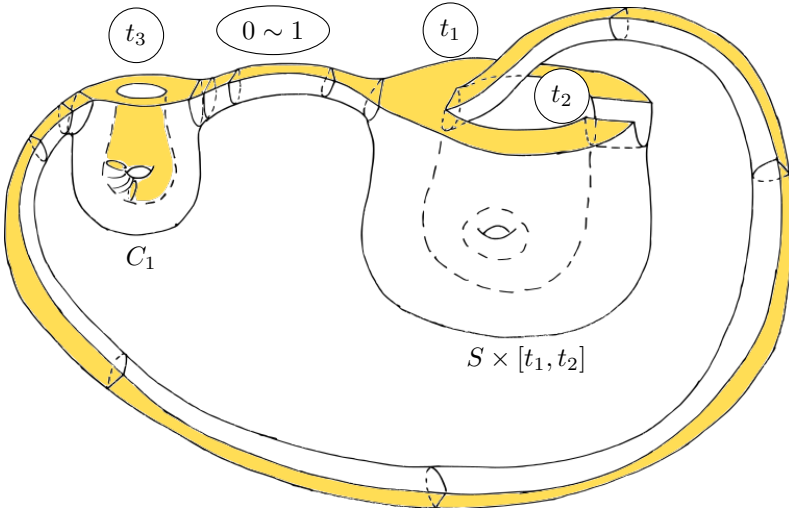


Figure 4.8. The page $(X_1 \cap X_2) \cap \partial X$, coloured in yellow on $X_1 \cap X_2$. Case 1.

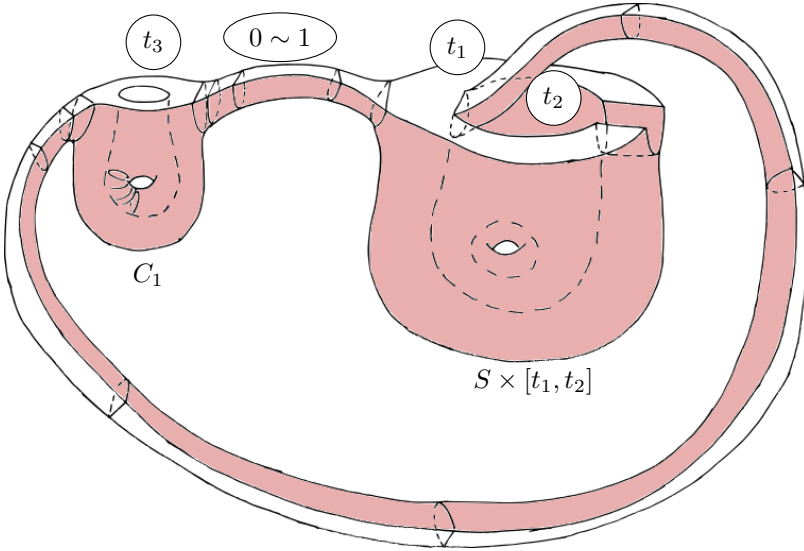


Figure 4.9. The central surface coloured in pink on $X_1 \cap X_2$. Case 1.

the sum of their number of boundary components; we write $c_{\mathcal{O}_k}$ the number of components of $\partial_- C_1$ (or equivalently of $\partial_- C_2$) in \mathcal{O}_k ;

- as ϕ also acts by permutation on the components of ∂S within each orbit, we write c_ϕ^k the number of induced orbits within a given \mathcal{O}_k , and $c_\phi = \sum_{k=1}^{\ell_X} c_\phi^k$ the total number of orbits of the action of ϕ on the components of ∂S .

Then X admits a $(G, k; P, B)$ -relative trisection, where:

- $G = 3g + 3b - c_\phi - 2$;
- $k = g + p + 2b - 1$;
- $P = (P_k)_{1 \leq k \leq \ell_X}$, with $P_k = p_k + b_k - c_{\mathcal{O}_k} - c_\phi^k + 1$;
- $B = (B_k)_{1 \leq k \leq \ell_X}$, with $B_k = 2c_\phi^k$.

The Euler characteristic of the central surface is given by $\chi = 3(\chi(S) - b)$.

Proof. — We only need to compute the parameters of the trisection defined in Proposition 4.4. Each X_i is a union of a $C_k \times I$ (a 4-dimensional handlebody of genus $g + p + b - 1$) and b 4-dimensional 1-handles. Therefore $k = g + p + 2b - 1$. To compute the genus and number of boundary components of the triple intersection and of the pages, we use their Euler

characteristic χ . Recall that gluing a band by two opposite edges on a triangulated surface S produces a surface S' with $\chi(S') = \chi(S) - 1$. As the central surface consists of three copies of S joined by $3b$ bands, we obtain that its Euler characteristic is $3(\chi(S) - b)$. Using the fact that we also have $\chi(F_{G,B}) = 2 - 2G - B$, we can derive G from χ just by counting the boundary components of the central surface. The monodromy acts on the boundary components of S by permutation. One orbit of this permutation creates exactly two boundary components of the central surface. So if we denote by c_ϕ the number of orbits of the permutation, we obtain that $B = 2c_\phi$, and that $G = 3g + 3b - c_\phi - 2$. The same applies to the genus P_k of each component of a page. One component is constituted of $c_{\mathcal{O}_k}$ components of a $\partial_- C_i$ that belong to the same orbit, joined by b_k bands, the resulting surface having $B_k = 2c_\phi^k$ boundary components. We get that $P_k = p_k + b_k - c_{\mathcal{O}_k} - c_\phi^k + 1$. \square

Example 4.6. — If the monodromy preserves all the boundary components of S and if the boundary of M is connected, we obtain a $(3g + 2b - 2, g + p + 2b - 1; p, 2b)$ -relative trisection of X .

4.2. Case 2: ϕ preserves a sutured Heegaard splitting of M

The process and notations are the same as in the previous case. We use a decomposition as shown on Figure 4.10. We will not reiterate the proof that this decomposition is indeed a relative trisection of X , as it is essentially the same as the proof of Proposition 4.4.

We just outline a few facts. Now the negative boundaries of the compression bodies are not necessarily diffeomorphic. Because we do need the pages $(X_i \cap X_j) \cap \partial X$ to be diffeomorphic, we split the interval I into six subintervals. Therefore the genus of the relative trisection will be higher than in Case 1, as the central surface will be constituted of six copies of S joined by bands. Note that the monodromy can still flip some boundary components of S or M .

THEOREM 4.7. — *Let M be a smooth, compact, oriented, connected 3-manifold and ϕ an orientation-preserving self-diffeomorphism of M . Let X be the smooth oriented bundle over the circle with fiber M and monodromy ϕ . The monodromy acts by permutation on the connected components $\{\partial^1 M, \dots, \partial^{\ell_M} M\}$ of ∂M , and we call $\sigma_{\phi, \partial M}$ this action. Let $M = C_1 \cup_S C_2$ be a sutured Heegaard splitting of M that is preserved by ϕ . We set the following notations:*

- *the surface S is of genus g with b boundary components;*
- *we write p_i the sum of the genera of the components of $\partial_- C_i$;*

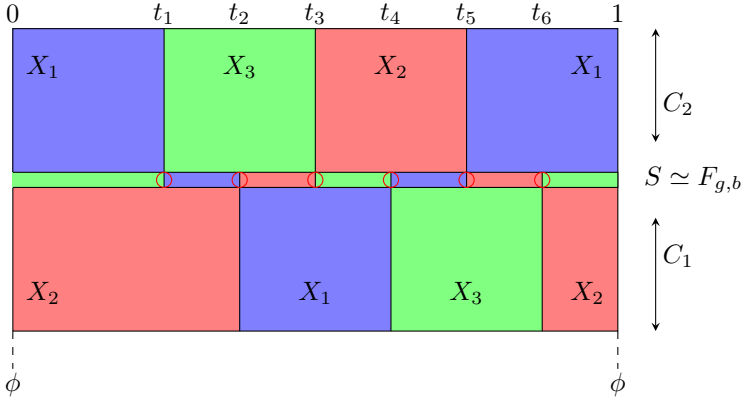


Figure 4.10. A relative trisection of X , Case 2.

- we denote the orbits of $\sigma_{\phi, \partial M}$ by $\{\mathcal{O}_1, \dots, \mathcal{O}_{\ell_X}\}$, where ℓ_X is the number of boundary components of X ; we write $p_{k,i}$ the sum of the genera of the components of $\partial_- C_i$ within \mathcal{O}_k and b_k the sum of their numbers of boundary components; we write $c_{\mathcal{O}_k,i}$ the number of components of $\partial_- C_i$ in \mathcal{O}_k ;
- as ϕ also acts by permutation on the components of ∂S within each orbit, we write c_{ϕ}^k the number of induced orbits within a given \mathcal{O}_k , and $c_{\phi} = \sum_{k=1}^{\ell_X} c_{\phi}^k$ the total number of orbits of the action of ϕ on the components of ∂S .

Then X admits a $(G, k; P, B)$ -relative trisection, where:

- $G = 6g + 6b - c_{\phi} - 5$;
- $k = 2g + p_1 + p_2 + 4b - 3$;
- $P = (P_k)_{1 \leq k \leq \ell_X}$, with $P_k = p_{k,1} + p_{k,2} + 2b_k - c_{\mathcal{O}_k,1} - c_{\mathcal{O}_k,2} - c_{\phi}^k + 1$;
- $B = (B_k)_{1 \leq k \leq \ell_X}$, with $B_k = 2c_{\phi}^k$.

The Euler characteristic of the central surface is given by $\chi = 6(\chi(S) - b)$.

Proof. — We just give a sketch of proof, as the arguments are essentially the same as those produced for Theorem 4.5. We can still compute the genus of this relative trisection using the Euler characteristic of the central surface. We obtain a central surface of Euler characteristic $6(\chi(S) - b)$, where $S \simeq F_{g,b}$ is the Heegaard surface of the splitting. Then we use the Euler characteristics of the components of the pages and the number of boundary components of the surfaces involved to compute the parameters featured in Theorem 4.7. \square

Example 4.8. — For instance, if the monodromy preserves all the boundary components of S and if the boundary of M is connected, we obtain a $(6g + 5b - 5, 2g + p_1 + p_2 + 4b - 3; p_1 + p_2 + b - 1, 2b)$ -relative trisection of X .

Remark 4.9. — In [13], Koenig builds trisections of the same (optimal) genus in both cases. His construction is less straightforward if the monodromy preserves a Heegaard splitting of M and the question of its adaptability to the compact setting is open.

5. The diagrams

Recall that X is a fiber bundle over S^1 , with fiber $M = C_1 \cup_S C_2$. Using a sutured Heegaard diagram of the fiber, we draw the diagrams corresponding to the relative trisections of Section 4, also considering the two separate cases.

5.1. A specific compression body

While constructing our relative trisections, we encountered a certain type of compression body, that we denote by $C_{g,b} = F_{g,b} \times I$, with:

- its positive boundary $\partial_+ C_{g,b}$ the union of $F_{g,b} \times \{0\}$ and $F_{g,b} \times \{1\}$, with matching boundary components joined two by two by bands;
- its negative boundary a disjoint union of b disks, each one capping off a boundary component of $\partial_+ C_{g,b}$.

We want to define a cut system on $\partial_+ C_{g,b}$ corresponding to this compression body. If an arc a is properly embedded in $F_{g,b}$, then $a \times I$ is a properly embedded disk in $C_{g,b}$, with boundary the curve $(a \times \{0\}) \cup (\partial a \times I) \cup (-a \times \{1\})$. By placing ∂a on a band joining $F_{g,b} \times \{0\}$ to $F_{g,b} \times \{1\}$, we ensure that the boundary of the disk lies on $\partial_+ C_{g,b}$. Therefore such a curve can be a candidate for our cut system.

Remark 5.1. — To draw our diagrams in the next figures, we choose an embedding of $\partial_+ C_{g,b}$ with $F_{g,b} \times \{0\}$ symmetric to $F_{g,b} \times \{1\}$: with this embedding, the curve on the previous discussion will be constituted of an arc on $F_{g,b} \times \{0\}$, connected to its symmetric on $F_{g,b} \times \{1\}$ by disjoint arcs drawn on the relevant band (or, informally, any curve on $\partial_+ C_{g,b}$ looking symmetric in $F_{g,b} \times \{0\}$ and $F_{g,b} \times \{1\}$ bounds a properly embedded disk in $C_{g,b}$).

We define the following cut system, represented on Figure 5.1:

- From $2g$ non isotopic and properly embedded arcs on $F_{g,b} \times \{0\}$, that cut the surface into a disk with $(b - 1)$ holes, we obtain $2g$ non isotopic curves on $\partial_+ C_{g,b}$ defined as above (in deep blue on Figure 5.1). After performing surgery along these curves, we are down to a surface of genus $(b - 1)$ with b boundary components.
- The previous step singled out a boundary component of $F_{g,b} \times \{0\}$ (in dotted light blue on Figure 5.1), whose glued on band was used to draw the $(\partial a \times I)$ part of the curves. We choose $(b - 1)$ arcs linking this component to the others, then draw the $(b - 1)$ curves obtained as above from these arcs (symmetric curves in green on Figure 5.1). After performing surgery along these curves, we obtain a sphere with b boundary components.
- We draw $(b - 1)$ curves, each one parallel to a boundary component (in red on Figure 5.1); surgery along these curves produces the b disjoint disks corresponding to $\partial_- C_{g,b}$.
- As all these curves bound properly embedded disks in $C_{g,b}$, we are done.

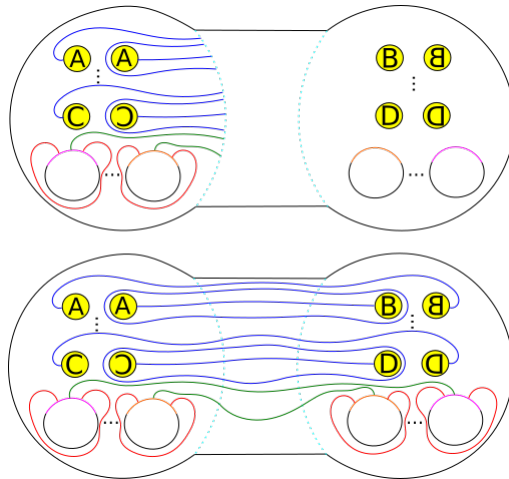


Figure 5.1. A cut system for $C_{g,b}$. The circles bounding yellow disks are identified two by two to contribute to the genus of each copy of $F_{g,b}$; the black semi-circles represent parts of the boundary components of each copy; the coloured semi-circles (here in pink or orange) are identified by colour to form the bands; we picked one component on which we drew the connecting arcs.

5.2. Relative trisection diagrams, Case 1

The monodromy flips a sutured Heegaard splitting of M , of which we use a sutured Heegaard diagram. Recall from Section 4 that the handlebodies $X_i \cap X_j$ are constituted of a copy of C_1 or C_2 and a handlebody $F_{g,b} \times I$, joined by 1-handles. The central surface is constituted of three copies of S joined by bands. The cut systems corresponding C_1 or C_2 can be derived from the sutured Heegaard diagram of M . We also need to obtain a compression body $F_{g,b} \times [t_k, t_{k+1}] \simeq C_{g,b}$ from the last two copies of S joined by bands. So we can use the results of Section 5.1, we choose the following embedding for the central surface. We label S_k the copy $S \times \{t_k\}$. We divide the plane equally, according to three rays, θ_1 , θ_2 and θ_3 . We draw S_k on θ_k , such that S_2 is the symmetric of S_1 along the ray midway between θ_1 and θ_2 , and the symmetric of S_3 along the ray midway between θ_2 and θ_3 (see Figure 5.2). The following algorithm produces a relative trisection diagram of X .

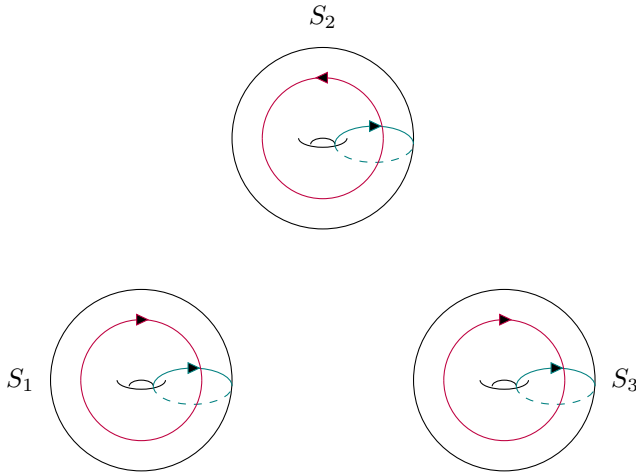


Figure 5.2. Symmetric embeddings of the copies of S in the central surface. Case 1.

- Start with the red curves associated to $X_1 \cap X_2$.
 - At t_3 , we have a copy of C_1 ; we draw the corresponding diagram on S_3 .
 - Between t_3 and t_1 , our compression body is just a thickening of the bands joining the copies of S , so we do not add any curve (the same applies between t_2 and t_3).

- From t_1 to t_2 , we have a copy of $C_{g,b}$; we draw the corresponding diagram on the union of S_2, S_3 and their linking bands, as in Section 5.1.
- Then we draw the blue curves corresponding to $X_1 \cap X_3$ in the same fashion, remembering that this time we have a copy of C_1 at t_1 and a copy of $C_{g,b}$ from t_2 to t_3 .
- We finish with the green curves corresponding to $X_2 \cap X_3$.
 - At t_2 , we have a copy of C_2 ; we draw the corresponding diagram on S_2 . Such a diagram is symmetric to a diagram drawn on S_1 or S_3 because of the embedding of the central surface.
 - Between t_2 and t_3 , our compression body is just a thickening of the bands joining the copies of S , so we do not add any curve (the same applies between t_1 and t_2).
 - From t_3 to t_1 , $X_2 \cap X_3$ consists in two compression bodies glued along part of their boundary, according to the monodromy ϕ . If we consider an arc a in S_1 , and its image $\phi(a)$ in S_3 , we can glue the two disks $(a \times [t_1, 0])$ and $(a \times [1, t_3])$ along $(a \times \{0\}) \simeq (\phi(a) \times \{1\})$. By doing so we obtain a disk in the quotient compression body, bounded by $(a \times \{t_1\}) \cup (\partial a \times [t_1, 0]) \cup_\phi (\partial a \times [1, t_3]) \cup (-\phi(a) \times \{t_3\})$. So if we provide a set of arcs on S_1 as in Section 5.1, we obtain, by gluing each arc to its image by ϕ on S_3 (with opposite direction), a cut system corresponding to the quotient compression body.

Notice that the red and blue curves do not depend on the monodromy. As we can always choose meridians and/or boundary parallel curves as a cut system for C_1 , the red and blue curves only depend on M to that extent. Figure 5.3 represents these curves when the cut system corresponding to C_1 consists in a single meridian. The following examples illustrate the construction of the green curves.

Example 5.2. — Consider $M = (S^2 \times I) \simeq B_3 \setminus \overset{\circ}{B}_1$, where $B_r \subset \mathbb{R}^3$ is the 3-ball of radius r centered at the origin. If we divide M along the xz plane, we get a sutured Heegaard splitting of M , $M = C_1 \cup_S C_2$, of genus 0, with Heegaard surface an annulus. Now define the monodromy ϕ as the composition of the rotation of angle π along the z axis and the reflection along the sphere of radius 2 centred at the origin. Then ϕ flips the sutured Heegaard splitting $M = C_1 \cup_S C_2$ and the boundary components of M and S . A diagram featuring the green curves corresponding to this example is drawn on Figure 5.4.

Example 5.3. — Consider a Heegaard diagram for the genus 1 Heegaard splitting $H_1 \cup_{T^2} H_2$ of the lens space $L(2, 1)$. Choose a disk disjoint from the curves on the diagram. Then the sutured Heegaard diagram obtained by

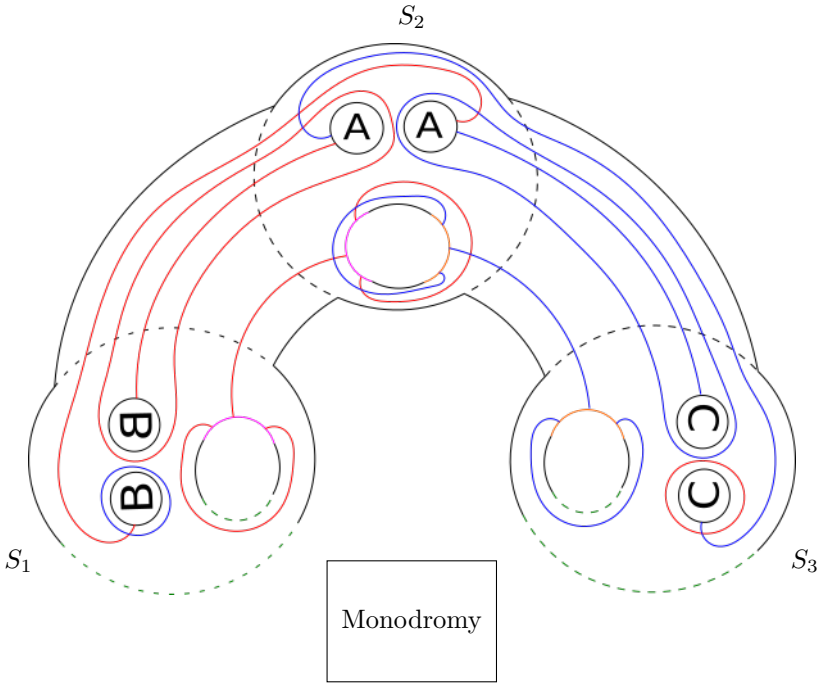


Figure 5.3. Sets of red and blue curves. Case 1. Here $S \simeq F_{1,2}$ and the cut system associated to C_1 is a single meridian; the way the dotted green arcs are identified depends on the monodromy.

removing the interior of the disk corresponds to $L(2, 1)$ minus the interior of a 3-ball B . We set this space as our fiber M . Let ϕ' be a diffeomorphism of T^2 that sends the meridian m to $-m + 2\ell$. Then ϕ' extends to a diffeomorphism of $L(2, 1)$, which flips the Heegaard splitting and preserves the 3-ball B . This diffeomorphism restricts to M and flips its sutured Heegaard splitting. We set it as our monodromy ϕ .

To draw the arcs defined in the algorithm above, we first isotope m and ℓ so that they meet the boundary of S_1 along two segments, then we remove those segments. We obtain two non-isotopic, properly embedded arcs drawn on S_1 . To get their images under the monodromy, we proceed in the same way with the images of the meridian and longitude: $\phi(m) = -m + 2\ell$ and $\phi(\ell) = \ell$. That gives us two oriented arcs on S_3 . As the image of an arc by the monodromy must be read with opposite direction to comply with the algorithm, we connect each arc on S_1 to its image on S_3 with reversed orientation.

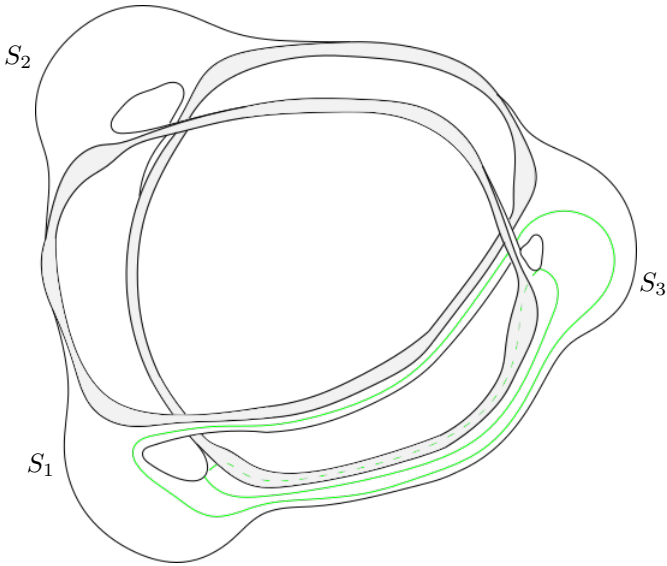


Figure 5.4. Set of green curves. Case 1, Example 5.2.

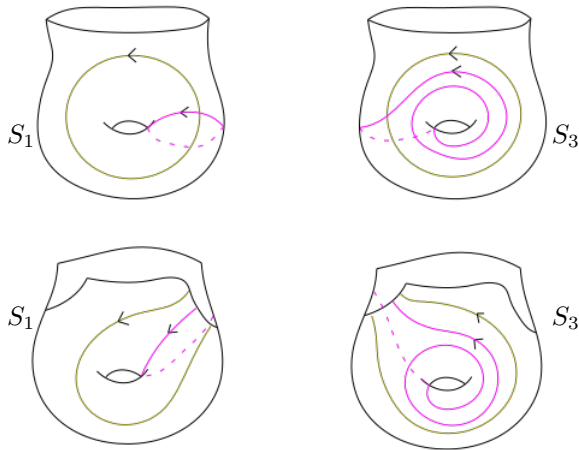


Figure 5.5. Finding the arcs on Example 5.3. Above: two essential oriented curves on S_1 and their oriented images on S_3 ; below: the oriented arcs obtained from these curves.

The green curves are displayed on Figure 5.6. Actually, this works for any lens space minus the interior of a 3-ball.

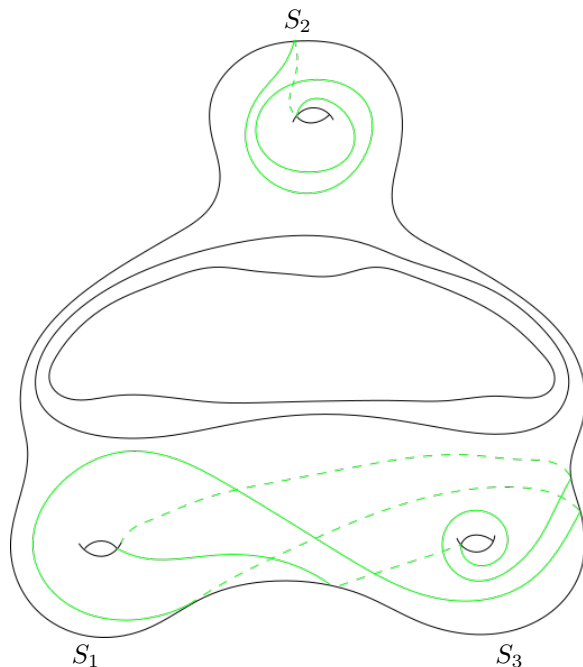


Figure 5.6. Green curves corresponding to Exemple 5.3. The curves on S_1 and S_3 are obtained from Figure 5.5 by connecting each arc on S_1 to its image with reversed orientation on S_3 ; the curve on S_2 is the symmetric of a curve $-m + 2\ell$ drawn on S_1 .

5.3. Relative trisection diagrams, Case 2

As we proceed essentially in the same way as in the previous case, we just outline the differences: we divide the plane in six sectors, using six rays θ_k from the origin; we draw one copy of S on each ray; we start with S_1 , then draw S_2 as its symmetric along a ray midway between θ_1 and θ_2 , and so on. With this choice of embedding, we can use the cut system for the product compression bodies $C_{g,b}$ defined in Section 5.1. Note that S_1 and S_6 , between which the monodromy occurs, are now symmetric, in contrast to Case 1. As the monodromy preserves the Heegaard splitting, we can get

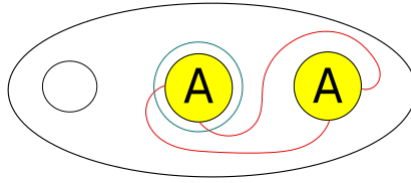


Figure 5.7. A sutured Heegaard diagram of the fiber.

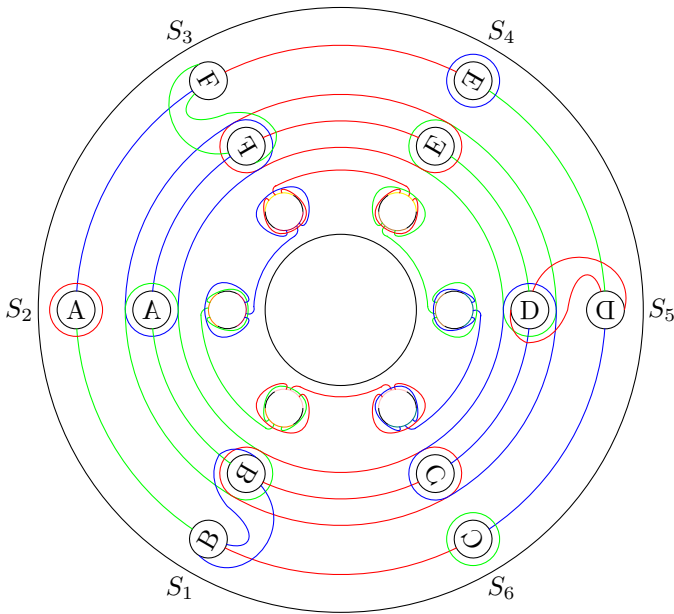


Figure 5.8. A relative trisection diagram of $X = S^1 \times M$, where M is defined by the sutured Heegaard diagram of Figure 5.7.

examples just by setting it to be the identity. Figure 5.8 represents a relative trisection diagram for $X = M \times S^1$, when the fiber M admits the sutured Heegaard diagram represented on Figure 5.7. If we take instead M to be a knot exterior in S^3 , we recover the relative trisection diagram for the product of a knot exterior with S^1 in [3].

Remark 5.4. — In [13], the trisection diagram obtained when the monodromy preserved the Heegaard splitting of the fiber could be destabilised. It would be interesting to see if the relative trisection diagram (of higher genus) obtained in the compact case can be destabilised as well.

6. Applications

Relative trisections can be combined to produce trisected closed manifolds. This aspect of the theory was developed in [4, 5]. In what follows, we consider only manifolds with connected boundaries. Our goal, in this section, is to use the results established in [5] in order to glue relatively trisected bundles over the circle to other relatively trisected 4-manifolds, thus producing classes of examples of trisected (closed) 4-manifolds. We recover the trisected closed bundles over the circle of [13], the trisected spun manifolds of [15], and we also provide trisections for some classes of 4-dimensional open-books.

6.1. Gluing relative trisection diagrams: theoretical aspects

DEFINITION 6.1. — *Let S be a compact surface and α a cut system of curves on S . Denote by S_α the surface obtained by surgering S along the α curves (that is, by cutting S along the α curves and gluing back a disk along every newly created boundary component). An arc system associated to α is a family of properly embedded arcs in S , such that cutting S_α along A_α produces a disk. We say that two cut systems together with their associated arcs (α, A_α) and $(\alpha', A_{\alpha'})$ are handleslide equivalent if one can be obtained from the other by sliding curves over curves and arcs over curves.*

DEFINITION 6.2. — *An arced diagram is a tuple $(S; \alpha, \beta, \gamma, A_\alpha, A_\beta, A_\gamma)$ such that:*

- $(S; \alpha, \beta, \gamma)$ is a relative trisection diagram;
- A_α (resp. A_β, A_γ) is an arc system associated to α (resp. β, γ);
- $(S; \alpha, \beta, A_\alpha, A_\beta)$ is handleslide equivalent to some $(S; \alpha', \beta', A_{\alpha'}, A_{\beta'})$, where $(S; \alpha', \beta')$ is diffeomorphic to a standard sutured Heegaard diagram D , and $A_{\alpha'} = A_{\beta'}$;
- $(S; \beta, \gamma, A_\beta, A_\gamma)$ is handleslide equivalent to some $(S; \beta', \gamma', A_{\beta'}, A_{\gamma'})$, where $(S; \beta', \gamma')$ is diffeomorphic to the same standard sutured Heegaard diagram D and $A_{\beta'} = A_{\gamma'}$.

Remark 6.3. — This intrinsic definition follows [8]. To explicitly draw an arced diagram from a relative trisection diagram, we apply the algorithm described in [3].

- Choose an arc system A_α associated to α .
- There is a collection of arcs A_β , obtained from A_α by sliding A_α arcs over α curves, and a set of curves $\tilde{\beta}$, obtained from β by handleslides, such that A_β and $\tilde{\beta}$ are disjoint.

- There is a collection of arcs A_γ , obtained from A_β by sliding A_β arcs over $\tilde{\beta}$ curves, and a set of curves $\tilde{\gamma}$, obtained from γ by handleslides, such that A_γ and $\tilde{\gamma}$ are disjoint.

Then $(S; \alpha, \tilde{\beta}, \tilde{\gamma}, A_\alpha, A_\beta, A_\gamma)$ is an arced diagram obtained from $(S; \alpha, \beta, \gamma)$.

That we can always find the advertised arcs and curves follows directly from the fact that (S, α, β) , (S, β, γ) and (S, α, γ) are standard. We make many choices when constructing the arcs and curves systems, but ([4]) these choices do not affect the final result: two arced diagrams obtained from the same relative trisection diagram are handleslide equivalent.

Remark 6.4. — The diagram $(S; \alpha, \beta, \gamma)$ describes a relatively trisected 4-manifold. The relative trisection induces an open-book decomposition of the boundary of the manifold, and the monodromy of this open-book can be explicitly computed using an associated arced diagram (see [3, 4]).

Let X and X' be relatively trisected compact 4-manifolds, with associated relative trisection diagrams $(S; \alpha, \beta, \gamma)$ and $(S; \alpha', \beta', \gamma')$, inducing the open book decomposition \mathcal{OB} on ∂X and \mathcal{OB}' on $\partial X'$. Suppose that there exists an orientation reversing diffeomorphism f from ∂X to $\partial X'$ that takes \mathcal{OB} to \mathcal{OB}' .

Construct an arced diagram $(S; \alpha, \tilde{\beta}, \tilde{\gamma}, A_\alpha, A_\beta, A_\gamma)$ from $(S; \alpha, \beta, \gamma)$. As $f(A_\alpha)$ cuts $S_{\alpha'} = f(S_\alpha)$ into a disk, construct an arced diagram $(S; \alpha', \tilde{\beta}', \tilde{\gamma}', A_{\alpha'}, A_{\beta'}, A_{\gamma'})$ from $(S, \alpha', \beta', \gamma')$, starting from $A_{\alpha'} = f(A_\alpha)$ and following the process described in Section 6.3.

Glue S and S' along their boundary, according to f . The process above associates to every arc in A_α (resp. A_β, A_γ) an arc in $A_{\alpha'}$ (resp. $A_{\beta'}, A_{\gamma'}$). Connect every arc to its associate, thus creating three families of curves $A_\alpha \cup A_{\alpha'}$, $A_\beta \cup A_{\beta'}$, $A_\gamma \cup A_{\gamma'}$ on $S \cup_f S'$.

THEOREM 6.5 (Castro–Gay–Pinzón–Caicedo). — *With the notations of the discussion above, $(S \cup_f S'; \alpha \cup \alpha' \cup (A_\alpha \cup A_{\alpha'}), \tilde{\beta} \cup \tilde{\beta}' \cup (A_\beta \cup A_{\beta'}), \tilde{\gamma} \cup \tilde{\gamma}' \cup (A_\gamma \cup A_{\gamma'}))$ is a trisection diagram for $X \cup_f X'$.*

Remark 6.6. — Proofs of Theorem 6.5 can be found in [3, 5]. More precisely, it is shown that gluing (g, k, p, b) and (g', k', p', b') relative trisections produces a $(g + g' + b - 1, k + k' - (2p + b - 1))$ -trisection of $X \cup_f X'$, in the case of connected boundaries.

6.2. Examples

We now use Theorem 6.5 to construct three classes of trisection diagrams from relative trisection diagrams. By doing so, we recover some trisections

diagram of [13, 15], and we also produce some classes of trisection diagrams of 4-dimensional open-books (for another approach on the subject, see [11]).

6.2.1. Koenig’s trisections of bundles over the circle

We consider a closed bundle over the circle of fiber M , where the monodromy preserves a genus g Heegaard splitting of the fiber. Consider the compact 3-manifold $M^\circ = M \setminus \text{Int}(B^3)$, where B^3 is a 3-ball transverse to the Heegaard surface of the splitting and preserved by the monodromy. Then the monodromy descends to M° and we obtain a bundle over S^1 of fiber M° , of which we can draw a relative trisection diagram as in Section 5. Actually, because the boundary of M° is just S^2 , we can use a lower genus (unbalanced) relative trisection of the bundle based on the schematic of Figure 6.2. An example of a relative trisection diagram corresponding to this decomposition is featured on Figure 6.3, with the associated systems of arcs (on the diagram, we assume the monodromy to be the identity, but this doesn’t affect our future considerations. We start from the Heegaard diagram for $L(2, 1)$ featured on Figure 6.1, left; by removing an open disk disjoint from the curves on the Heegaard surface, we obtain a sutured Heegaard diagram for $L(2, 1)^\circ$). To obtain our closed bundle over the circle of fiber M , we must glue back in a relatively trisected $S^1 \times B^3$, of which an arced diagram is just a cylinder with three parallel arcs as in Figure 6.4. As the pages and arcs defined by these diagrams agree, all we need to do is to glue the two arced diagrams together according to the identity. We obtain a $(4g + 1)$ -trisection diagram of the closed bundle (see Figure 6.5), equivalent to the diagram featured in [13]. This diagram can be destabilised g times to obtain $(3g + 1)$ -trisection diagram (for that last point, see [13]).

6.2.2. Meier’s trisections of spun manifolds

Let M be a closed 3-manifold and $M^\circ = M \setminus \text{Int}(B^3)$. The spun of M is defined as $\mathcal{S}(M) = (M^\circ \times S^1) \cup_{S^2 \times S^1, \text{Id}} (S^2 \times D^2)$. We proceed as in the previous example to draw a sutured Heegaard diagram for M° from a genus g Heegaard diagram for M . Then we apply the procedure defined in Section 5.3 to obtain a relative trisection diagram for $M^\circ \times S^1$, and finally an arced diagram for $M^\circ \times S^1$ (an example is featured on Figure 6.6, using the Heegaard diagram for $M \simeq L(2, 1)$ on Figure 6.1, right). An arced diagram for $S^2 \times D^2$ is featured on Figure 6.7 (see [3]). As the pages and arcs of these diagrams agree, we can glue them to obtain a $(6g + 3)$ -trisection diagram for $\mathcal{S}(M)$. Interestingly, we can explicitly modify this diagram through

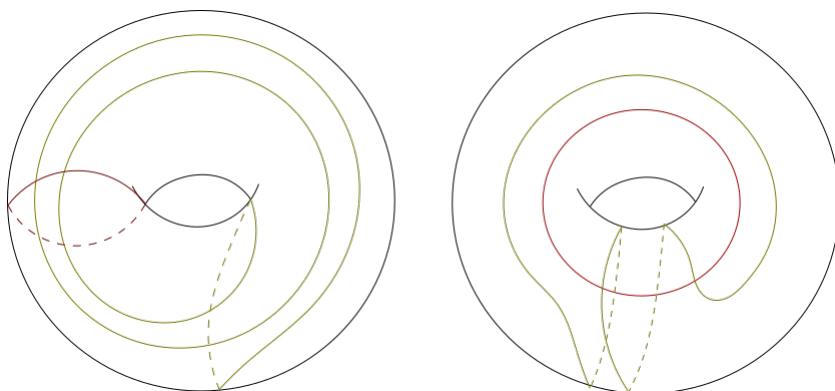


Figure 6.1. Two Heegaard diagrams for $L(2, 1)$.

X_1	X_2	X_1
X_3	X_1	X_3

Figure 6.2. A trisection of the bundle over S^1 of fiber M° .

handleslides and three destabilizations to obtain a diagram that is just the initial relative diagram of $M^\circ \times S^1$ with two disks capping off its boundary components (see Figure 6.8 for an example). Then we can further modify this trisection diagram through handleslides and $3g$ destabilisations to obtain the diagram featured in [15].

6.2.3. Trisections of some 4-dimensional open-books

Let M be a compact 3-manifold with boundary a torus, and ϕ a self-diffeomorphism of M that is the identity on a regular neighbourhood of ∂M . We define the 4-dimensional open-book of fiber M and monodromy ϕ as:

$$\mathcal{OB}(M) = ((M \times I)/\sim) \cup_{\partial M \times S^1, \text{Id}} (\partial M \times D^2), \text{ where } (x, 0) \sim (\phi(x), 1).$$

We prove the following.

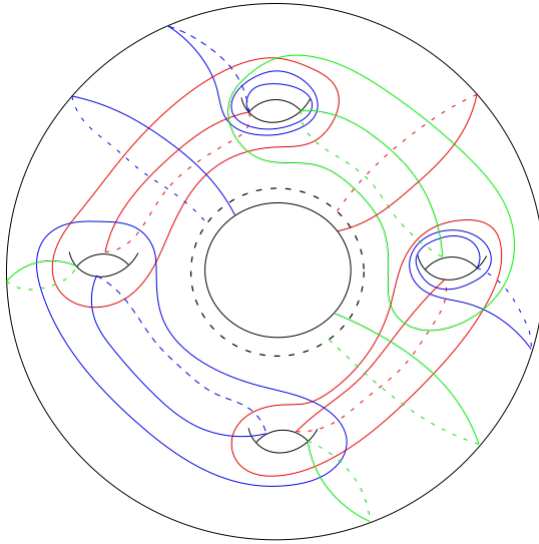


Figure 6.3. A genus 4 arced diagram for $S^1 \times M^o$, when $M \simeq L(2, 1)$.

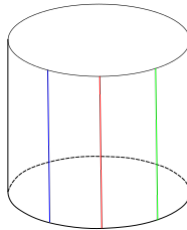


Figure 6.4. An arced diagram for $S^1 \times B^3$.

THEOREM 6.7. — *Let $\mathcal{OB}(M)$ be a 4-dimensional open-book of fiber M and monodromy ϕ , where M is a compact manifold with boundary a torus. Then there exists a sutured Heegaard splitting of M , preserved by ϕ , that induces a decomposition of ∂M as $\partial M = (\partial M \setminus \dot{D}) \cup D$, with D a disk in ∂M . Further, $\mathcal{OB}(M)$ admits a $(6g+4)$ -trisection, where g is the genus of this sutured Heegaard splitting of M . Moreover, a trisection diagram for $\mathcal{OB}(M)$ can be explicitly derived from a sutured Heegaard diagram corresponding to this splitting.*

Proof. — To produce a trisection of $\mathcal{OB}(M)$, we glue an arced diagram for the bundle $((M \times I)/\sim)$ to an arced diagram of $T^2 \times D^2$ from [5] (see Figure 6.9). The first diagram is obtained from a sutured Heegaard diagram of

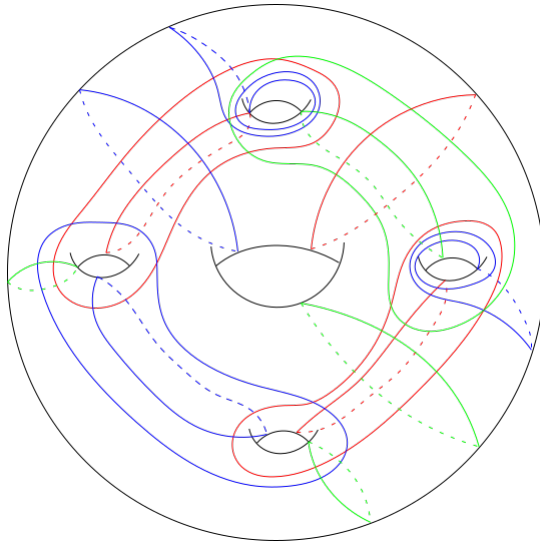


Figure 6.5. A trisection diagram for $S^1 \times M$, when $M \simeq L(2, 1)$.

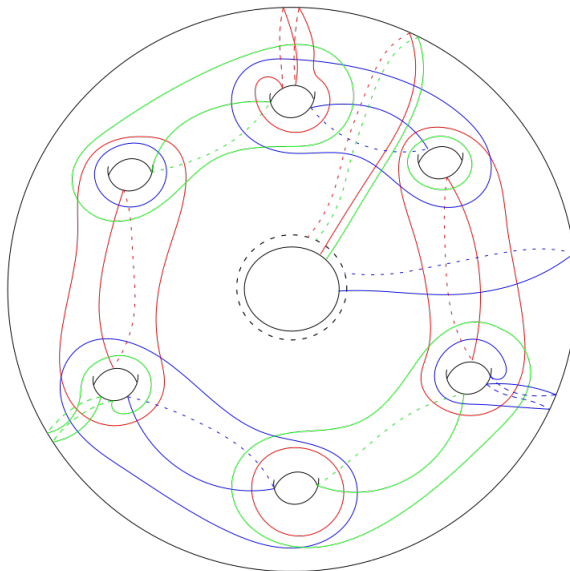


Figure 6.6. A genus 6 arced diagram for $S^1 \times M^o$, when $M \simeq L(2, 1)$.

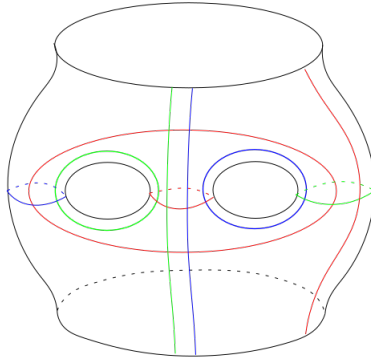


Figure 6.7. An arced diagram for $S^2 \times D^2$. We made some handleslides of arcs to prepare for the future destabilizations of the glued diagram.

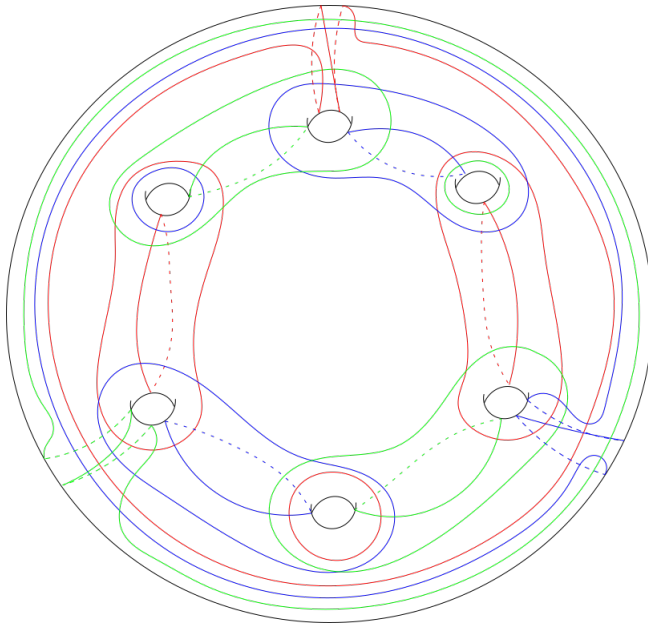


Figure 6.8. A trisection diagram for $\mathcal{S}(M)$, when $M \simeq L(2, 1)$.

M that induces the decomposition on the boundary of M : $\partial M = (\partial M \setminus \mathring{D}) \cup D$, where D is a disk in ∂M . An example of a sutured diagram verifying this condition is featured on Figure 6.10. The condition on the sutured Heegaard splitting allows the pages of the open-book decompositions of $((M \times I)/\sim)$

and $T^2 \times D^2$ to be diffeomorphic. Note that, because ϕ is the identity on a neighborhood of ∂M , it preserves any sutured decomposition of ∂M , therefore this specific sutured Heegaard splitting always exists (see Theorem 1.1). We obtain a relative trisection diagram with page a torus with two holes and compute a system of arcs that matches the one featured on Figure 6.9 (an example of the resulting diagram is drawn on Figure 6.11). Then we glue the two diagrams according to the identity, thus constructing a trisection diagram for $\mathcal{OB}(M)$ (see Figure 6.12 for an example; as the genus of the surfaces involved is quite high, we used this time a more suitable planar representation of these surfaces). While constructing the system of arcs of the relative trisection diagram for the bundle, one can check that it does not depend on the monodromy, nor on M (in our figures, we took the monodromy to be the identity). Therefore we have produced a $(6g + 4)$ -trisection diagram of $\mathcal{OB}(M)$, from a sutured Heegaard splitting of M of genus g . \square

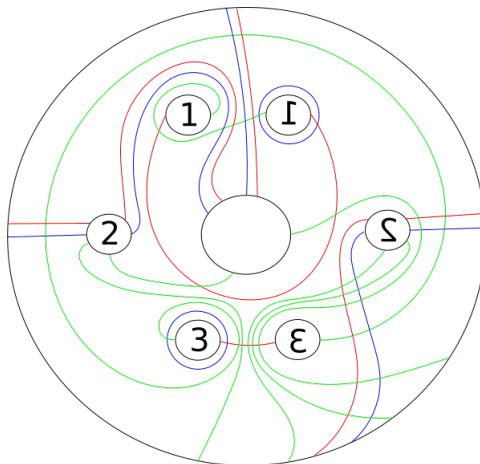


Figure 6.9. An arced diagram for $T^2 \times D^2$

Remark 6.8. — We do not know if the diagram obtained on Figure 6.12 might be destabilised to produce a lower genus trisection. It is shown in [11] that the trisection genus of our diagrams is not minimal.

Remark 6.9. — This method can be extended to produce a trisection diagram for *any* 4-dimensional open-book (without restricting the number of boundary components of the fiber or their genus). One has to check the compatibility of the pages induced by the relative trisections of the bundle over S^1 (of fiber M) and the bundle over ∂M (of fiber D^2), but this can always be achieved. To see this, consider first that ∂M is a connected surface of genus h . Then (see [3]), $\partial M \times D^2$ admits a $(h + 2, 2h + 1; h, 2)$ -relative

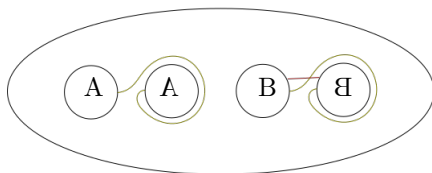


Figure 6.10. A sutured Heegaard splitting for some M with boundary a torus. To construct such an example, consider a Heegaard diagram, with the handlebody corresponding to the α curves standardly embedded in \mathbb{R}^3 , then puncture the Heegaard surface next to an α curve and remove this curve.

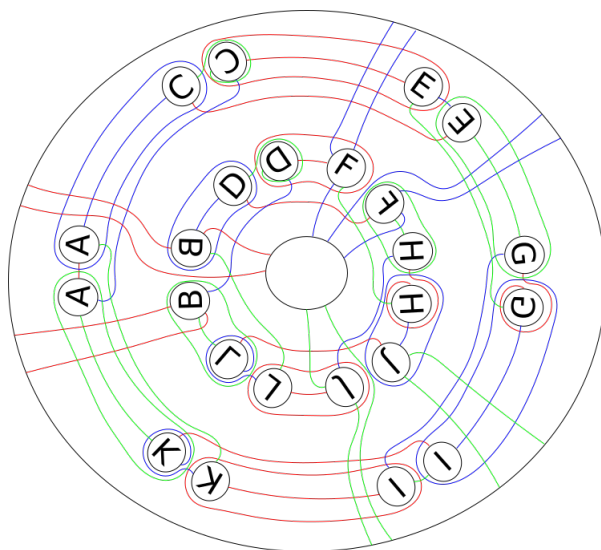


Figure 6.11. An arced diagram for $(M \times I)/\sim$, obtained from the diagram on Figure 6.10.

trisection. But (Theorem 4.7), the bundle $(M \times I)/\sim$ admits a $(6g + 5b - 5, 2g + p_1 + p_2 + 4b - 3; p_1 + p_2 + b - 1, 2b)$ -relative trisection, where ∂M admits a sutured decomposition between two surfaces of genus p_1 and p_2 with b boundary components. Therefore, to obtain diffeomorphic pages on the induced open-book decompositions of the boundaries of the two bundles, we need $b = 1$ and $p_1 + p_2 = h$, which can always be achieved by starting from a sutured decomposition $\partial M = (\partial M \setminus \text{Int}(D)) \cup D$, where D is a disk

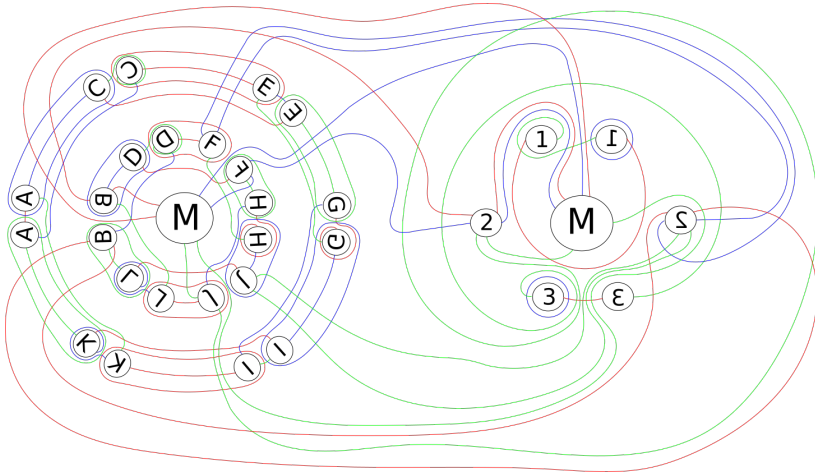


Figure 6.12. A trisection diagram for the open-book $\mathcal{OB}(M)$, obtained from the diagram on Figure 6.10.

embedded in ∂M . Using Remark 6.6, we can compute that we have obtained a $(6g+h+3, 2g+h+1)$ -trisection of $\mathcal{OB}(M)$, where h is the genus of ∂M and g the genus of the sutured Heegaard splitting of M . Then we could extend to the case where ∂M is not connected by applying this method to every boundary component.

Bibliography

- [1] M. BORODZIK, A. NÉMETHI & A. RANICKI, “Morse theory for manifolds with boundary”, *Algebr. Geom. Topol.* **16** (2016), no. 2, p. 971-1023.
- [2] N. A. CASTRO, “Relative trisections of smooth 4-manifolds with boundary”, PhD Thesis, University of Georgia, Athens, USA, 2016.
- [3] N. A. CASTRO, D. T. GAY & J. PINZÓN-CAICEDO, “Diagrams for relative trisections”, *Pac. J. Math.* **294** (2018), no. 2, p. 275-305.
- [4] ———, “Trisections of 4-manifolds with boundary”, *Proc. Natl. Acad. Sci. USA* **115** (2018), no. 43, p. 10861-10868.
- [5] N. A. CASTRO & B. OZBAGCI, “Trisections of 4-manifolds via Lefschetz fibrations”, 2017, <https://arxiv.org/abs/1705.09854>.
- [6] D. GABAI, “Foliations and the topology of 3-manifolds”, *Bull. Am. Math. Soc.* **8** (1983), no. 1, p. 77-80.
- [7] D. T. GAY & R. KIRBY, “Trisecting 4-manifolds”, *Geom. Topol.* **20** (2016), no. 6, p. 3097-3132.
- [8] D. T. GAY & J. MEIER, “Doubly pointed trisection diagrams and surgery on 2-knots”, *Math. Proc. Camb. Philos. Soc.* **172** (2022), no. 1, p. 163-195.
- [9] G. ISLAMBOULI, “Nielsen equivalence and trisections”, *Geom. Dedicata* **214** (2021), no. 1, p. 303-317.

- [10] A. JUHÁSZ, “Holomorphic discs and sutured manifolds”, *Algebr. Geom. Topol.* **6** (2006), no. 3, p. 1429-1457.
- [11] M. KEGEL & F. SCHMÄSCHKE, “Trisecting a 4-dimensional book into three chapters”, *Geom. Dedicata* **218** (2024), no. 4, article no. 86.
- [12] S. KIM & M. MILLER, “Trisections of surface complements and the Price twist”, *Algebr. Geom. Topol.* **20** (2020), no. 1, p. 343-373.
- [13] D. KOENIG, “Trisections of 3-manifold bundles over S^1 ”, *Algebr. Geom. Topol.* **21** (2021), no. 6, p. 2677-2702.
- [14] A. A. KOSINSKI, *Differential manifolds*, Academic Press Inc., 2013.
- [15] J. MEIER, “Trisections and spun 4-manifolds”, 2017, <https://arxiv.org/abs/1708.01214>.
- [16] J. MEIER & A. ZUPAN, “Genus two trisections are standard”, *Geom. Topol.* **21** (2017), no. 3, p. 1583-1630.
- [17] M. WILLIAMS, “Trisections of flat surface bundles over surfaces”, PhD Thesis, University of Nebraska-Lincoln, Lincoln, USA, 2020.